Journal of Pharmaceutical Innovation (2019) 14:132–140
https://doi.org/10.1007/s12247-018-9341-1

ORIGINAL ARTICLE

Development of Chitosan and Alginate Nanocapsules to Increase the Solubility, Permeability and Stability of Curcumin

Daniel Hernandez-Patlan[1] · Bruno Solis-Cruz[1] · Mario Alberto Cano-Vega[1,2] · Eric Beyssac[3] · Ghislain Garrait[3] · Xochitl Hernandez-Velasco[4] · Raquel Lopez-Arellano[1] · Guillermo Tellez[5,6] · Gustavo R. Rivera-Rodriguez[1]

Published online: 14 August 2018

Abstract

Purpose Curcumin (CUR), a natural polyphenolic compound, has several pharmacological uses, primarily regarding its anti-inflammatory, chemotherapeutic, and antioxidant properties. However, to date, a significant drawback of curcumin is its poor bioavailability due to its low solubility and permeability. Therefore, the association of curcumin in polymeric nanocapsules may be an excellent strategy to increase its bioavailability.

Methods Two nanocapsule systems were developed with an oily core of vitamin E surrounded by a biodegradable polymeric shell of either chitosan (NC-CS) or alginate (NC-ALG) capable of improving the encapsulation efficiency, stability, and permeability of CUR. NC-CS and NC-ALG showed particle sizes of approximately 116.7 ± 3.2 and 178 ± 7.9 nm, dispersities of 0.107 and 0.149, and zeta potentials of 24.4 ± 2.1 and − 49.0 ± 2.3 mV, respectively.

Results The encapsulation efficiency was approximately 90% in both cases, and they were demonstrated to be stable under storage conditions for 3 months. Cytotoxicity studies performed in Caco-2 cells using the method of trypan blue dye revealed that even at a high concentration of chitosan and alginate (157.9 μg/cm^2 or 600 mg/mL), both of the nanocapsules were not toxic, exhibiting cell viability > 80%. The permeability was evaluated using Caco-2 cells as an in vitro model of the epithelial barrier. The obtained results show that the permeability of NC-CS and NC-ALG encapsulated CUR was considerably higher compared to that of an aqueous suspension.

Conclusions The obtained results suggest that nanocapsules could improve the solubility, permeability, and stability of curcumin.

Keywords Curcumin · Permeability · Polymeric nanocapsules · Solubility · Stability

✉ Guillermo Tellez
gtellez@uark.edu

[1] Laboratorio 5: LEDEFAR, Unidad de Investigación Multidisciplinaria, Facultad de Estudios Superiores Cuautitlán, Universidad Nacional Autonoma de Mexico, 54714 Cuautitlan Izcalli, Estado de Mexico, Mexico

[2] Department of Agricultural and Biological Engineering, Purdue University, West Lafayette, IN 47907, USA

[3] Université Clermont Auvergne, INRA, UMR MEDIS, 63000 Clermont-Ferrand, France

[4] Departamento de Medicina y Zootecnia de Aves, Facultad de Medicina Veterinaria y Zootecnia, Universidad Nacional Autonoma de Mexico, 04510 Ciudad de Mexico, Mexico

[5] Department of Poultry Science, University of Arkansas, Fayetteville, AR 72710, USA

[6] JKS Poultry Health Laboratory, 2652 N. McConnell Ave., Fayetteville, AR 72704, USA

Introduction

Curcumin (CUR) or diferuloylmethane, a yellow polyphenolic substance and the principal curcuminoid of turmeric (*Curcuma longa*), has been widely used in the food and chemical industry as coloring, flavoring, and preservative. Furthermore, it has been reported that CUR is a potent natural antioxidant [1, 2] and an anti-inflammatory agent [3–5] and has therapeutic potential in metabolic and autoimmune diseases, such as type II diabetes, multiple sclerosis, Alzheimer's disease, Parkinson's disease, and atherosclerosis [6–11]. Additionally, CUR has chemopreventive and anti-cancer activities [12, 13].

Despite all of CUR's aforementioned pharmacological properties, it exhibits extremely poor water solubility, which results in a low absorption of this drug by the gastrointestinal tract [14] and therefore a poor bioavailability, even if administered at a dose of 12 g/day [15].

In vivo studies have shown that after oral administration of CUR, most of the CUR is excreted in the feces, and although it was not detected in urine, several of its derivatives, such as curcumin glucuronide and sulfates, were observed, indicating that this phytopharmaceutical undergoes rapid metabolization in the liver and is rapidly removed from systemic circulation [14]. Furthermore, it is also known that CUR is unstable at neutral-basic pH values and in serum-free mediums, since it is degraded to vanillin, ferulic acid, feruloyl methane, and trans-6-(40-hydroxy-30-methoxy-phenyl)-2,4-dioxo-5-hexenal [16].

In this sense, the association of CUR in nanocapsule systems is a strategy to solve its problems of solubility, permeability, and stability, since it has been reported that the incorporation of therapeutic agents in polymer matrices, particularly biocompatible and biodegradable ones, such as chitosan and alginate, might potentiate the protection of the biologically active compound from degradation, control the drug release, and improve solubility, absorption, and its therapeutic effect [17].

Chitosan (CS) is a cationic biopolymer that has been widely used for the delivery of various therapeutic agents associated with CS micro- and nanoparticles, due to its unique properties. Several applications of this biopolymer are the preparation of mucoadhesive formulations, enhancing the dissolution rate, especially for poorly water-soluble drugs, the utilization of drug targeting, and the improvement of protein absorption [18]. CS is insoluble in water; in neutral or basic pH conditions, it is positively charged. In an acidic pH, amino groups can undergo protonation, thus making it soluble in water. Nevertheless, the solubility of CS also depends on the distribution of free amino and *N*-acetyl groups [18, 19].

In contrast, alginate (ALG) is an anionic biopolymer used to prepare nanocapsules due to its excellent biocompatibility, biodegradability, non-toxicity, mucoadhesion, gelation, and film formation properties [20]. ALG is a polysaccharide consisting of D-mannuronic acid and L-guluronic acid arranged as blocks in a polymeric chain. It is known that at a low pH, the release of the encapsulated material is stopped due to the formation of an insoluble layer. However, at a higher pH, it becomes a soluble viscous layer, releasing the encapsulated material [21]. Alginate has been widely studied for particle formation in size range of 100 nm to 2 mm for drug delivery, but it has not been used for the formulation of nanocapsules containing a volatile oily drug [21].

In the present study, two nanocapsule systems were developed with an oily core of vitamin E surrounded by a biodegradable polymeric shell of either chitosan (NC-CS) or alginate (NC-ALG) capable of improving the encapsulation efficiency, stability, and permeability of CUR.

Materials and Methods

Chemicals

Curcumin ≈ 70% (CUR) (Sigma-Aldrich®, Mexico), Poloxamer 188 (Pluronic® F68, Sigma Chemical Co., USA), cetyltrimethylammonium bromide (CTAB) (Sigma-Aldrich®, France), sodium alginate (ALG) (Manucol® DH, ISP, Germany), chitosan (CS) (mol wt 50,000–160,000 Da, 75–85% deacetylated, Sigma-Aldrich®, Mexico), vitamin E (α-tocopherol, Sigma-Aldrich, Switzerland), Cremophor® EL (BASF, Germany), polysorbate 80 (Acros Organics, USA), and acetic acid (CH_3COOH, Sigma-Aldrich, Germany).

Preparation of NC-CS

Nanocapsules with a polymeric coating of CS were prepared using a slightly modified solvent displacement technique [22]. Briefly, the formation of the nanocapsules is based on the electrostatic and hydrophobic interactions that occur between the chitosan dissolved in an acidic aqueous phase and the lipid cores of vitamin E formed in the organic phase. The organic phase was formed by dissolving 0.015 g CUR in 800 μL ethanol followed by the addition of 200 μL vitamin E, 120 μL Cremophor® EL, and 5 mL acetone. This organic phase was immediately poured into 20 mL of a polymeric solution of CS (0.025 g) with a 5% stoichiometric excess of acetic acid and 0.06 g of poloxamer 188. The polymer solution was prepared by dissolving the CS in 2 mL acetic acid 0.1 N under stirring for 15 min and was subsequently increased to a volume of 20 mL with distilled water. Finally, the solvents are removed from the nanosuspension under vacuum until a final volume of 20 mL is achieved.

Preparation of NC-ALG

NC-ALG were obtained by a modification of the solvent displacement technique described by Rivera-Rodriguez (2013), which consists of the "single-stage procedure" given the dipolar ionic interactions between the polymer (ALG), which is dissolved in the aqueous phase, and the cationic surfactant (CTAB) present in the organic phase, which also contains the oil (vitamin E). The organic phase was formed by dissolving 0.005 g of the cationic surfactant and 0.015 g of CUR in 800 μL of ethanol, followed by the addition of 200 μL vitamin E, 120 μL Cremophor® EL, and 5 mL acetone. This organic phase was immediately poured into 20 mL the aqueous phase containing 0.06 g of poloxamer 188 and 0.030 g ALG under mild stirring. When the ALG interacts with the cationic surfactant, a polymeric coating is formed at the oil/water interface, thereby forming the alginate nanocapsules (NC-ALG).

Finally, the solvents are removed from the nanosuspension under vacuum until a final volume of 20 mL is achieved.

Characterization of CS and ALG Nanocapsules

NC-CS and NC-ALG were characterized regarding their size, zeta potential, and morphology. The particle size and polydispersity index (PDI) were determined by dynamic light scattering (DLS) after dilution of nanocapsules in deionized water, and each analysis was carried out at 25 °C with an angle detection of 173°. The zeta potential values were calculated from the mean electrophoretic mobility values, as determined by laser Doppler velocimetry (LDV). For the LDV measurements, samples were diluted in the same way as for the determination of the particle size. Samples were loaded into a Malvern DTS1060 capillary cuvette. The DLS and LDV analyses were performed on three independently prepared samples using a Zetasizer Nanoseries 3600 (Malvern Instruments, Worcestershire, UK). The morphology was determined using transmission electron microscopy.

CUR Encapsulation Efficiency

The quantification of the CUR was carried out using high-performance liquid chromatography (HPLC, Merck-Hitachi, Japan). The HPLC system was equipped with a DAD detector and a reverse phase Hypersil® Division C8 column (150 mm × 3 mm, 5 μm; ThermoQuest, Hemel Hempstead, England). CUR was detected at a wavelength of 425 nm. The mobile phase consisted of a mixture of 55% deionized water and 45% acetonitrile with a constant flow rate of 0.5 mL/min. The injection volume of the samples was 80 μL.

The CUR encapsulation efficiency was determined indirectly by centrifugation-filtration. To determine the amount of non-encapsulated CUR, 1 mL of the nanocapsule formulation was diluted with 4 mL of deionized water and centrifuged at 15,000 rpm for 20 min (Centrifuge 2-16P, SIGMA, Fisher Bioblock Scientific, Germany). Subsequently, an aliquot of 1 mL of the supernatant was taken and diluted with 4 mL of deionized water. This last dilution of the formulation was filtered two times (Millipore 0.2 and 0.1 μm) and diluted with 5 mL of the mobile phase. The total amount of CUR was estimated by dissolving 1 mL of the formulation of the nanocapsules in 10 mL acetonitrile followed by centrifugation at 15,000 rpm for 10 min.

The encapsulation efficiency (EE) for CUR was calculated as follows:

$$\mathrm{EE}(\%) = \frac{(A-B)}{A} \times 100$$

where A is the total concentration of CUR in the formulation and B is the concentration of free curcumin measured in the aqueous external medium, corresponding to the non-encapsulated curcumin.

Stability Studies

Stability of nanocapsules was evaluated under storage conditions at 4 °C for 3 months. The parameters assessed were (1) particle size, (2) zeta potential, and (3) polydispersity index (PDI).

Cell-Based Studies

Caco-2 Cell Culture

The Caco-2 human colon cancer cells from the American Type Culture Collection (ATCC, Rockville, MD) at passage 16 were cultured in T-75 cm^2 flasks containing Dulbecco's modified Eagle medium (DMEM, Gibco-Invitrogen, Fisher, Illkirch, France) supplemented with glucose (4.5 g/L), FBS (15%; *v*/*v*), vitamins (2%; *v*/*v*), nonessential amino acid solution (2%; *v*/*v*), L-glutamine (2%; *v*/*v*), and antibiotic solution (2%; *v*/*v*), at 37 °C in a humidified atmosphere of 5% CO_2/95% air. When the cell culture reached 80–90% confluence, cells were dispersed with 0.025 M trypsin-EDTA and reseeded in a new flask. The culture medium was changed every 3 days. For cell viability assay, cells were seeded onto 12-well plates (3.8 cm^2, Well Plates Corning®, Kennebunk, EU) at a density of 5×10^4 cells per well and cultured for 21 days. For permeability studies, cells were seeded on the apical side of Transwell® permeable supports (Transwell Corning®, Kennebunk, EU, 0.4 μm polycarbonate membrane, 1.12 cm^2 surface, and a volume of 0.5 mL in the apical compartment and 1.5 mL in the basolateral compartment) at a density of 2×10^4 cells per well for 21 days. In both studies, the culture medium was changed every 3 days.

MTT Cell Viability Assay

Formulation of nanocapsules was diluted in DMEM to get polymeric concentrations of 125, 250, and 500 μg/mL (equivalents in dose per unit area of 32.9, 65.8, and 131.6 μg/cm^2) and curcumin concentrations of 75 μg/mL, 150, and 300 μg/mL (equivalents in dose per unit area of 19.7, 39.4, and 78.8 μg/cm^2), whereas for curcumin alone, it was suspended in DMEM and then diluted to get the different concentrations of curcumin (125, 250, and 500 μg/mL or 32.9, 65.8, and 131.6 μg/cm^2). After differentiation (21st day), the culture medium was removed, and 1 mL of each dilution of the formulation was taken and placed in each of the wells in triplicates ($n = 3$). Cells were exposed for a period of 2 h. After 1 h of incubation, 5 μL MTT solution (5 mg/mL) was added to each well and incubated for 1 h more to complete 2 h in a humidified atmosphere of 5% CO_2/95% air at 37 °C. Next, the

supernatant was removed and 1 mL of isopropanol (Sigma-Aldrich Co.) solution containing 0.04 N HCl (Sigma-Aldrich Co.) and 0.1% nonidet P-40 (Fluka Chemical Corp., Buchs., Switzerland) was added to each well before reading their optical density at 590 nm in a single cell Life Science UV-Vis Spectrophotometer Model DU530 (Beckman-Coulter Inc., Brea, CA, USA). The experiment was performed at least three times.

Permeability Studies

Permeability studies were also performed after complete cell differentiation, and only wells exhibiting transepithelial electrical resistance (TEER, MERSSTX01 electrode, Millicell ERS-2, Millipore, Billerica, MA, USA) greater than 600 Ω cm^2 were used. Before starting the experiment, the culture medium was removed, and cell monolayers were washed twice with 1 mL of PBS buffer. Then, 0.5 mL of the formulations diluted with a concentration of 250 μg/mL was added to the apical side of the cell monolayers, while on the basolateral side, 1.5 mL of DMEM was placed. Cells were incubated at 37 °C for 120 min. Every 60 min, the TEER was measured, and the total volume of the basolateral side was taken and replaced by fresh DMEM. Passage of the CUR was determined by UPLC-TQ-ESI-MS/MS (Waters ACQUITY UPLC system, Milford, MA, USA). The chromatographic analysis was performed on a Waters ACQUITY BEH Shield RP 18 column (2.1 × 100 mm, 1.7 μm). The mobile phase was composed of 60% A (acetonitrile and 0.1% formic acid) and 40% B (0.1% formic acid solution). The flow rate of the mobile phase was 0.25 mL/min, and the injection volume was 7.5 μL. The column temperature was conditioned at 30 °C, and the autosampler was maintained at 4 °C. At the end of the experiment, the permeability studies were stopped by removing the apical medium and washing the cells three times with PBS. Immediately, the samples were replaced with fresh medium that had been incubated at 37 °C. The monolayers were allowed to regenerate for 24 h at 37 °C in a humidified atmosphere of 5% CO_2/95% air.

Results are expressed as apparent permeability coefficient (Papp) and variation of the TEER (%) compared to the initial values, calculated according to the following equations:

$$\text{TEER}\ (\%) = \frac{(\text{TEER}_t)}{(\text{TEER}_{t0})} \times 100$$

$$\text{Papp}\ (\text{cm/s}) = \left(\frac{dQ}{dt}\right) \times \left(\frac{1}{A \times C_0}\right)$$

Results and Discussion

In the present work, the development of two nanocapsule systems with an oily core of vitamin E surrounded by a biodegradable polymeric shell of CS or ALG is described. These nanocapsule systems were designated NC-CS and CN-ALG and were characterized physicochemically in terms of the particle size, zeta potential, and polydispersity index (PDI). Furthermore, the stability was evaluated, and the toxicity and permeability studies were performed on Caco-2 cells, the latter with the purpose of determining how much the nanocapsule systems increase the permeability of the CUR with respect to raw CUR. This type of nanocapsule systems has gained considerable importance in recent years due to its multiple advantages, including the increase in the stability of the drug encapsulated against biological media and during storage, passive targeting or more extended systemic circulation, and the solubility improvement of highly lipophilic drugs due to the use of oil cores.

Characterization of NC-CS and NC-ALG

Both formulations containing CUR were prepared according to the solvent displacement technique and characterized for their size, polydispersity index (PDI), pH, zeta potential, and encapsulation efficiency (Table 1). The results show that the polydispersion indexes of NC-CS and NC-ALG are 0.107 and 0.149, respectively, which indicate that NC-CS formed more homogeneous populations (a narrow distribution) compared to NC-ALG since the polydispersity index is closer to 0.1 [22]. The particle size of NC-CS was approximately 116.7 nm and presented a positive surface charge (24.4 mV) while NC-ALG was about 178 nm with a negative surface charge (− 49.0 mV). Transmission electron microscopy (TEM) micrographs of these nanocapsule systems are shown in Fig. 1 and corroborate the particle size.

The CUR encapsulation efficiency of both formulations was > 90%, with a final concentration of CUR of approximately 750 μg/mL. The high CUR encapsulation efficiency was mainly due to the preparation method and the properties of the oil core [23]. Nevertheless, the maximum solubility of the active substance in the oil is one of the most important criteria for the selection of the base forming oil and the concentration of the active material during the development of this type of formulation [24]. Therefore, vitamin E was selected to form the core of the nanocapsules since curcumin presents a good solubility in it.

Stability Studies

Several factors can affect the stability of nanocapsule systems, for example, the composition of nanocapsules, the conditions,

Table 1 Physicochemical characteristics of the nanocapsule systems obtained. PDI: polydispersity index; EE: encapsulation efficiency

Formulation	Particle size (nm)	PDI	ζ potential (mV)	EE (%)	pH
NC-NC	116.7 ± 3.2	0.107	24.4 ± 2.1	> 98	4.67 ± 0.08
NC-ALG	178 ± 7.9	0.149	− 49.0 ± 2.3		6.08 ± 0.06

Values are given as mean ± SD; $n = 3$

and methods of preparation and storage. Nevertheless, it is difficult to identify the specific factors.

An easy way to identify if a nanocapsule system is unstable is through examining its visual aspects, such as color and the presence of aggregates, but it is also necessary to determine certain physicochemical elements, such as the particle size, pH, and quantification of the active substance.

Table 2 shows the results obtained in terms of the particle size, PDI, and zeta potential after maintaining the nanocapsule systems (NC-CS and NC-ALG) at a temperature of 4 °C (storage conditions). In both formulations, the particle size, PDI value, and zeta potential were slightly modified. In the case of the NC-CS, the stability of these formulations was approximately 3 months from the initial experiment; the decrease in the particle size and the precipitation of the CUR were presented with a greater magnitude. This finding may be attributable to the fact that chitosan begins to hydrolyze slowly (breaking of the chitosan chains) during the storage period given the pH of the formulation and therefore the viscosity decreased, making it more susceptible to suffer physical stability problems [25, 26]. Although an increase in PDI values is related to the degradation of the polymer and the aggregation or presence of the binding of particles, the value obtained after 3 months was 0.196 and indicates that there is a narrow size distribution (homogeneous population) since the PDI value is between 0.1 and 0.2 [27, 28]. Furthermore, the zeta potential remained at approximately 24 mV such that electrostatic repulsion was maintained between the particles, minimizing the likelihood of aggregation [29] at least during the 3 months of the study.

However, the stability of NC-ALG was slightly lower than that of NC-CS due to the decrease in particle size is greater after the second month. These results are similar to other studies where it has been reported that between months 1 and 5, the decrease of the particle size is more marked and is followed by a phase where the difference in the particle size is less than 1 nm from months 5 to 12 [25]. Unlike CS, ALG is stable in the pH range of 5 to 10 [30]. Nevertheless, at a neutral or alkaline pH, ALG forms a soluble viscous layer and starts to release the encapsulated material [21], causing a decrease in the particle size given the dissolution of the alginate matrix [31]. In this case, the polydispersity index after 3 months of storage was higher than 0.2 and indicates that the dispersion is less homogeneous than that of NC-CS. Additionally, there was a decrease in the zeta potential, which is indicative that the system was less stable due to the possible aggregation of the particles [29].

Cell Viability Assay

An important parameter when assessing the potential of a new nanoparticulate drug delivery system is its cellular toxicity.

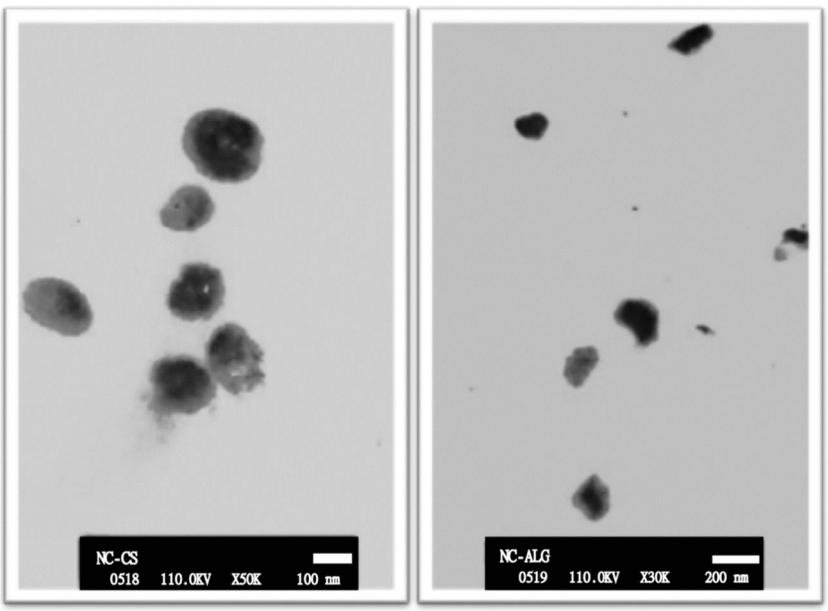

Fig. 1 Transmission electron microscopy micrographs, scale bar, represents 100 nm for NC-CS (**a**) and 200 nm for NC-ALG (**b**)

Table 2 Physicochemical characteristics of chitosan nanocapsules (NC-CS) and alginate nanocapsules (NC-ALG) during stability studies under storage conditions (4 °C)

Formulation	Time (months)	Particle size (nm)	PDI	ζ potential (mV)
NC-CS	0	116.7 ± 3.2	0.107	24.4 ± 2.1
	1	115.2 ± 2.9	0.115	23.8 ± 2.1
	2	101.3 ± 4.1	0.145	23.9 ± 3.2
	3	95.45 ± 3.0	0.196	24.5 ± 2.8
NC-ALG	0	178 ± 7.9	0.149	− 49.0 ± 2.3
	1	161.9 ± 2.1	0.178	− 48.7 ± 1.9
	2	157.7 ± 4.77	0.213	− 46.8 ± 2.5
	3	149.3 ± 2.9	0.245	− 44.3 ± 2.7

Values are given as the mean ± SD; $n = 3$

PDI polydispersity index

The viability of the Caco-2 cells after being exposed and incubated for 2 h at 37 °C with the two formulations considering different polymer concentrations is shown in Fig. 2. The results show that even at a polymer concentration of 500 μg/mL (131.6 μg/cm^2), the cell viability was above 80%, which indicates that these nanocapsule systems are not toxic; however, the toxicity increases as the polymer concentration does. Nevertheless, the cell viability was higher for NC-ALG than NC-CS at the same level. These differences in toxicity are mainly due to the characteristics of the polymer such as the molecular weight and surface charge since they are critical parameters for the interaction with cell membranes and consequently cell damage [28]. On the other hand, the particle size has also been identified as a primary parameter in the increase of the toxicity of different materials [32].

Previous studies in Caco-2 cells have shown that the toxicity of CS nanoparticles depends on the molecular weight of CS, the concentration to which the cells are exposed and the physicochemical properties of these nanosystems, such as the size and the surface charge [28, 29, 33]. This last parameter is essential since it is related to cellular damage due to the strong ionic interaction that can be carried out between the amino groups of CS and the cell membrane [30]. Nevertheless, in the case of ALG, these interactions are weaker since they are of the electrostatic type between the carboxyl groups of ALG and the cell membranes, causing the toxicity to be mainly related to the particle size [31].

Effect of NC-CS, NC-ALG, and CUR on TEER

TEER is a parameter that provides a measure of the barrier properties of the epithelium and its integrity [32, 34]. Furthermore, this parameter is frequently used as a sensitive marker of cell damage, indicating toxicity or suggesting a change in the epithelial barrier function [35, 36].

Modifications in the membrane permeability are usually associated with a reduction in TEER values due to the opening of *tight junctions* [37]. TEER measurements were made at 0, 60, and 120 min after the exposure of NC-CS, NC-ALG, CUR, and DMEM (control) on the Caco-2 cell monolayer. After the last TEER measurement, the above systems were removed, and the cells were washed three times with PBS. Immediately, the fresh culture medium was placed to verify if the TEER values were recovered after 24 h. Figure 3 shows that NC-CS and NC-ALG decreased the TEER value to approximately 81 and 88%, respectively, while the TEER values for CUR and DMEM were above 90%. This decrease in the TEER values indicates the opening of *tight junctions*.

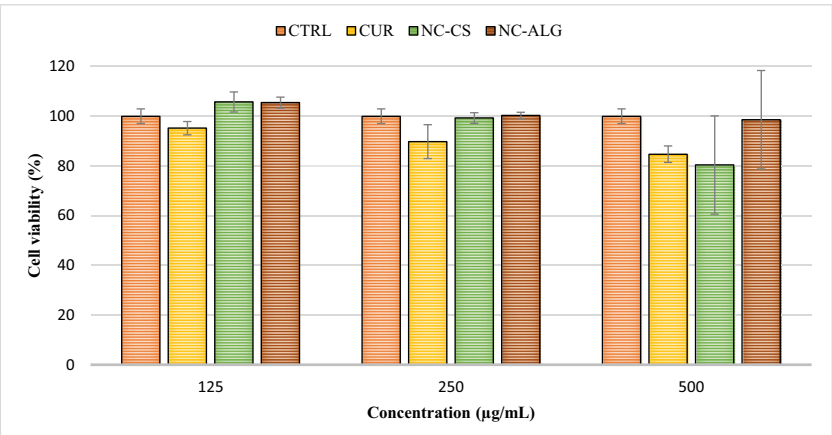

Fig. 2 Cell viability by the MTT assay on Caco-2 cells 2 h after the addition of chitosan nanocapsules (NC-CS), alginate nanocapsules (NC-ALG), and curcumin (CUR) at different concentrations. Values are given as mean ± SD; $n = 3$

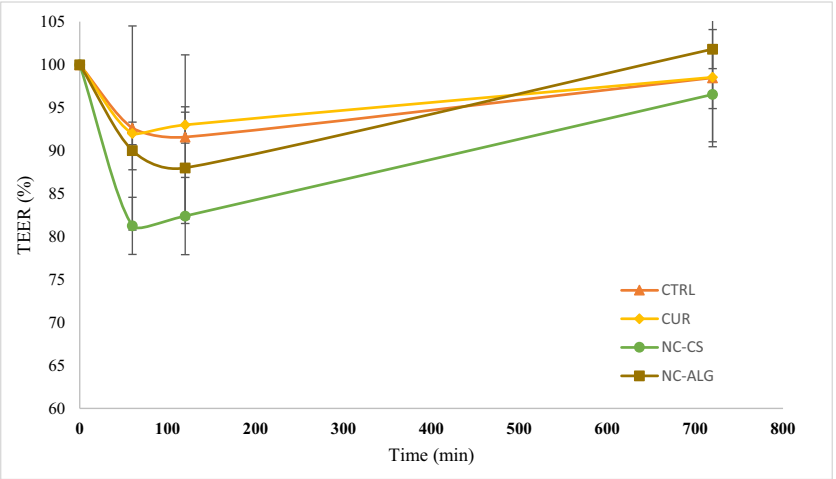

Fig. 3 Effect of chitosan nanocapsules (NC-CS) or alginate nanocapsules (NC-ALG) (dose per unit area of 32.9 μg/cm^2 or 125 mg/mL of polymer in both cases), curcumin (CUR) (dose per unit area of 32.9 μg/cm^2 or 125 μg/mL), and Dulbecco's modified eagle medium (CTRL) on the values of transepithelial electrical resistance (TEER) as a function of time. Values are given as mean ± SD; $n = 3$

However, 24 h after the NC-CS and NC-ALG were removed, the initial value of the TEER was recovered, meaning that the disturbance of the monolayer is transient. Considering that the concentration of N-CS and CN-ALG (125 μg of polymer per well or 111.6 μg/cm^2 in both cases) used does not compromise the cell viability, the reduction in the TEER could be associated directly with the capacity of NC-CS and NC-ALG to open *tight junctions* temporarily.

Determination of Apparent Permeability

The permeability of an active coating on a monolayer of Caco-2 cells depends mainly on its concentration, exposure time, and temperature. Therefore, each of these factors was homogenized in order not to overestimate the results. Table 3 shows the mean apparent permeability (Papp) and the absorption enhancement ratio (R) of NC-CS, NC-ALG, and CUR across the Caco-2 cell monolayers. In the case of nanocapsule systems, the concentration used was 250 μg/mL of each polymer and a CUR concentration of 150 μg/mL (equivalent to 125 μg of polymer and 75 μg of CUR per well or 111.6 and 67.0 μg/cm^2, respectively) and CUR of 250 μg/mL (equivalent to 125 μg/mL of CUR per well or 111.6 μg/cm^2), that is, the cell viability was not compromised since it was higher than 80% according to the results of Fig. 2. The results show that the permeability of CUR increased 28.6 and 14.6 times when it was in NC-CS and NC-ALG, respectively, compared to the dispersion of curcumin in DMEM (CUR).

The increase in the permeability of CUR in NC-CS is due to the ability of CS to temporarily open *tight junctions*, thus allowing an increase in the permeability of active compounds, since it acts as a promoter of absorption and the rise in the solubility of the CUR. The mechanism by which CS has this capacity is based on the interaction of its protonated amino groups with cell membranes. This interaction produces a reversible structural reorganization of the binding proteins and a specific redistribution of the actin F cytoskeleton and the ZO-1 protein (present in the *tight junctions*), which leads to the opening of the *tight junctions* and thus the increase in paracellular transport [38–41]. Another mechanism is related to the interactions between the amino groups of CS and the membrane proteins that are negatively charged to form clathrin vesicles and that once in the cytoplasm can bind with the endosome/lysosome compartments to break the chemical bonds and structure of the particles by the acidity of the medium or enzymes to release the active compound. Furthermore, it has been seen that positively charged particles with a spherical shape and with a monodisperse population have improved cellular uptake through the caveolae-mediated endocytosis and macropinocytosis pathway [42–45]. In this sense, the permeability of CUR in NC-CS is higher given the combination of internalization mechanisms. Meanwhile, the interaction of ALG with the cell membrane is weaker due to its negative charge at the pH of the culture medium (≈ 7.2), such that the mechanism of passage through the monolayer of Caco-2 cells depends mainly on the particle size mainly since it has been reported that particle sizes between 100 and 200 nm utilize paracellular transport mechanisms [46]. Nevertheless, NC-ALG also utilizes internalization mechanisms by endocytosis, such as clathrin-mediated endocytosis, caveolae-mediated endocytosis, and micropinocytosis [45, 47].

Table 3 Mean apparent permeability (Papp) and the absorption enhancement ratio (R) of chitosan nanocapsules (NC-CS), alginate nanocapsules (NC-ALG), and curcumin across Caco-2 cell monolayers after 2-h incubation

Formulation	Papp × 10^{-6} (cm/s)	R
CUR	4.96 ± 0.36	–
NC-CS	141.60 ± 37.62	28.6*
NC-ALG	72.38 ± 19.33	14.6*

Values are given as the mean ± SD; $n = 3$

*Significantly different from curcumin $P < 0.05$

Conclusions

The results of the present study show that the permeability of curcumin increases 28.6 and 14.6 times when it was in NC-CS and NC-ALG, respectively, compared to raw curcumin, suggesting that the bioavailability of curcumin could be increased. Nevertheless, the permeability of curcumin was higher when it was encapsulated in NC-CS due to the smaller particle size and by the combination of paracellular and transcellular passage mechanisms through the monolayer of the Caco-2 cells compared to NC-ALG. However, it is also necessary to consider that the solubility of curcumin in these nanosystems was increased due to the oily core and the surfactants used. Furthermore, NC-CS were observed to be more stable under storage conditions than NC-ALG. Therefore, these systems could be an essential strategy to improve the solubility, permeability, and stability of curcumin.

Acknowledgments This research was supported by the Arkansas Bioscience Institute under the project: Development of an avian model for evaluation early enteric microbial colonization on the gastrointestinal tract and immune function.

Author Contributions Daniel Hernández-Patlán, Bruno Solís-Cruz, Mario Alberto Cano-Vega, Eric Beyssac, Ghislain Garrait, Guillermo Tellez, Raquel López-Arellano, and Gustavo R. Rivera-Rodriguez contributed to the overall study design and supervised all research. Daniel Hernández-Patlán, Bruno Solis-Cruz, and Mario Alberto Cano-Vega carried out the experiments and acquisition of data. Daniel Hernández-Patlán, Gustavo R. Rivera-Rodriguez, and Guillermo Tellez drafted and revised the first version of the manuscript. Daniel Hernández-Patlán, Bruno Solís-Cruz, Eric Beyssac, Ghislain Garrait, Raquel López-Arellano, Guillermo Tellez, and Gustavo R. Rivera-Rodriguez analyzed the data. Xochitl Hernandez-Velasco, Guillermo Tellez, and Gustavo R. Rivera-Rodriguez drafted the article and revised it critically for important intellectual content. Daniel Hernández-Patlán, Xochitl Hernandez-Velasco, and Guillermo Tellez were also responsible for the final editing of the manuscript. All the authors reviewed and finally approved the manuscript.

Funding Information The authors thank the CONACyT for the doctoral scholarship number 447447 and the financial support obtained through the program PAPIIT IN218115 of DGAPA-UNAM.

Compliance with Ethical Standards

Conflicts of Interest The authors declare that they have no conflict of interest.

References

1. Ak T, Gülçin İ. Antioxidant and radical scavenging properties of curcumin. Chem Biol Interact. 2008;174:27–37. Available from: http://www.sciencedirect.com/science/article/pii/S0009279708002573
2. Priyadarsini IK. The chemistry of curcumin: from extraction to therapeutic agent. Molecules. 2014;19:20091–112.
3. Began G, Sudharshan E, Appu Rao AG. Inhibition of lipoxygenase one by phosphatidylcholine micelles-bound curcumin. Lipids Germany. 1998;33:1223–8.
4. Chan MM-Y, Huang H-I, Fenton MR, Fong D. In vivo inhibition of nitric oxide synthase gene expression by curcumin, a cancer preventive natural product with anti-inflammatory properties. Biochem Pharmacol. 1998;55:1955–62. Available from: http://www.sciencedirect.com/science/article/pii/S0006295298001142
5. Menon VP, Sudheer AR. In: Aggarwal BB, Surh Y-J, Shishodia S, editors. Antioxidant and anti-inflammatory properties of curcumin—the molecular targets and therapeutic uses of curcumin in health and disease. Boston: Springer US; 2007. p. 105–25. Available from: https://doi.org/10.1007/978-0-387-46401-5_3.
6. Wongcharoen W, Phrommintikul A. The protective role of curcumin in cardiovascular diseases. Int J Cardiol. 2009;133:145–51. Available from: http://www.sciencedirect.com/science/article/pii/S0167527309001132
7. Hamaguchi T, Ono K, Yamada M. REVIEW: curcumin and Alzheimer's disease. CNS Neurosci Ther England. 2010;16:285–97.
8. Mythri RB, Bharath MMS. Curcumin: a potential neuroprotective agent in Parkinson's disease. Curr Pharm Des Netherlands. 2012;18:91–9.
9. Maradana MR, Thomas R, O'Sullivan BJ. Targeted delivery of curcumin for treating type 2 diabetes. Mol Nutr Food Res Germany. 2013;57:1550–6.
10. Sahebkar A. Dual effect of curcumin in preventing atherosclerosis: the potential role of pro-oxidant–antioxidant mechanisms. Nat Prod Res [Internet]. Taylor & Francis; 2015;29:491–2. Available from: https://doi.org/10.1080/14786419.2014.956212.
11. Wanninger S, Lorenz V, Subhan A, Edelmann FT. Metal complexes of curcumin—synthetic strategies, structures, and medicinal applications. Chem Soc Rev [Internet]. The Royal Society of Chemistry; 2015;44:4986–5002. Available from: https://doi.org/10.1039/C5CS00088B
12. López-Lázaro M. Anticancer and carcinogenic properties of curcumin: considerations for its clinical development as a cancer chemopreventive and chemotherapeutic agent. Mol Nutr Food Res. Wiley Online Library; 2008;52.
13. Tuorkey M. Curcumin a potent cancer preventive agent: mechanisms of cancer cell killing. Interv Med Appl Sci Akadémiai Kiadó. 2014;6:139–46.
14. Mazzarino L, Dora CL, Bellettini IC, Minatti E, Cardoso SG, Lemos-Senna E. Curcumin-loaded polymeric and lipid nanocapsules: preparation, characterization and chemical stability evaluation. Lat Am J Pharm. 2010;29:933–40.
15. Anand P, Kunnumakkara AB, Newman RA, Aggarwal BB. Bioavailability of curcumin: problems and promises. Mol Pharm ACS Publications. 2007;4:807–18.
16. Lin C-C, Lin H-Y, Chen H-C, Yu M-W, Lee M-H. Stability and characterization of phospholipid-based curcumin-encapsulated microemulsions. Food Chem Elsevier. 2009;116:923–8.
17. Ahmed TA, Aljaeid BM. Preparation, characterization, and potential application of chitosan, chitosan derivatives, and chitosan metal nanoparticles in pharmaceutical drug delivery. Drug Des Devel Ther. Dove Press; 2016;10:483.
18. Agnihotri SA, Mallikarjuna NN, Aminabhavi TM. Recent advances on chitosan-based micro-and nanoparticles in drug delivery. J Control Release Elsevier. 2004;100:5–28.
19. Szymańska E, Winnicka K. Stability of chitosan—a challenge for pharmaceutical and biomedical applications. Mar Drugs Multidiscip Digital Publish Inst. 2015;13:1819–46.
20. Lertsutthiwong P, Noomun K, Jongaroonngamsang N, Rojsitthisak P, Nimmannit U. Preparation of alginate nanocapsules containing turmeric oil. Carbohydr Polym. 2008;74:209–14. Available from:

http://www.sciencedirect.com/science/article/pii/S0144861708000817
21. Natrajan D, Srinivasan S, Sundar K, Ravindran A. Formulation of essential oil-loaded chitosan-alginate nanocapsules. J food drug Anal Elsevier. 2015;23:560–8.
22. Suhaimi SH, Roslic NA. Effects of formulation parameters on particle size and polydispersity index of Orthosiphon stamineus loaded nanostructured lipid carrier. J Adv Res Appl Sci Eng Technol. 2015;1:36–9.
23. Khayata N, Abdelwahed W, Chehna MF, Charcosset C, Fessi H. Preparation of vitamin E loaded nanocapsules by the nanoprecipitation method: from laboratory scale to large scale using a membrane contactor. Int J Pharm. 2012;423:419–27. Available from: http://www.sciencedirect.com/science/article/pii/S0378517311011422
24. Fresta M, Cavallaro G, Giammona G, Wehrli E, Puglisi G. Preparation and characterization of polyethyl-2-cyanoacrylate nanocapsules containing antiepileptic drugs. Biomaterials. 1996;17:751–8. Available from: http://www.sciencedirect.com/science/article/pii/0142961296814116
25. Vårum KM, Smidsrød O. Structure-property relationship in chitosans. In: Polysaccharides: structural diversity functional versatility. New York: Marcel Dekker; 2005. p. 625–42.
26. Rokhati N, Widjajanti P, Pramudono B, Susanto H. Performance comparison of α - and β-amylases on chitosan hydrolysis. ISRN Chem Eng. 2013;2013:186159.
27. Danhier F, Lecouturier N, Vroman B, Jerome C, Marchand-Brynaert J, Feron O, et al. Paclitaxel-loaded PEGylated PLGA-based nanoparticles: in vitro and in vivo evaluation. J Control Release Netherlands. 2009;133:11–7.
28. Thipparaboina R, Chavan RB, Shastri NR. Nanocrystals for delivery of therapeutic agents. Part Technol Deliv Ther. Springer; 2017. p. 291–316.
29. Maruyama CR, Guilger M, Pascoli M, Bileshy-José N, Abhilash PC, Fraceto LF, et al. Nanoparticles based on chitosan as carriers for the combined herbicides imazapic and imazapyr. Sci Rep. Nat Publ Group. 2016;6:19768.
30. Guarino V, Caputo T, Altobelli R, Ambrosio L. Degradation properties and metabolic activity of alginate and chitosan polyelectrolytes for drug delivery and tissue engineering applications. Aims Press; 2015;
31. Marković D, Zarubica A, Stojković N, Vasić M, Cakić M, Nikolić G. Alginates and similar exopolysaccharides in biomedical application and pharmacy: controlled delivery of drugs. Adv Technol. 2016;5:39–52.
32. Fröhlich E, Roblegg E. Models for oral uptake of nanoparticles in consumer products. Toxicology Elsevier. 2012;291:10–7.
33. Ma H, Qi X, Maitani Y, Nagai T. Preparation and characterization of superparamagnetic iron oxide nanoparticles stabilized by alginate. Int J Pharm [Internet]. 2007;333:177–86. Available from: http://www.sciencedirect.com/science/article/pii/S0378517306008131
34. Huang M, Khor E, Lim L-Y. Uptake and cytotoxicity of chitosan molecules and nanoparticles: effects of molecular weight and degree of deacetylation. Pharm Res United States. 2004;21:344–53.
35. Schipper NG, Varum KM, Artursson P. Chitosans as absorption enhancers for poorly absorbable drugs. 1: influence of molecular weight and degree of acetylation on drug transport across human intestinal epithelial (Caco-2) cells. Pharm Res United States. 1996;13:1686–92.
36. Prego C, Fabre M, Torres D, Alonso MJ. Efficacy and mechanism of action of chitosan nanocapsules for oral peptide delivery. Pharm Res. United States. 2006;23:549–56.
37. Fischer D, Li Y, Ahlemeyer B, Krieglstein J, Kissel T. In vitro cytotoxicity testing of polycations: influence of polymer structure on cell viability and hemolysis. Biomaterials Netherlands. 2003;24:1121–31.
38. Pasternak AS, Miller WM. Measurement of trans-epithelial electrical resistance in perfusion: potential application for in vitro ocular toxicity testing. Biotechnol Bioeng United States. 1996;50:568–79.
39. Van der Lubben IM, Verhoef JC, Borchard G, Junginger HE. Chitosan and its derivatives in mucosal drug and vaccine delivery. Eur J Pharm Sci [Internet]. 2001;14:201–7. Available from: http://www.sciencedirect.com/science/article/pii/S0928098701001725
40. Amidi M, Mastrobattista E, Jiskoot W, Hennink WE. Chitosan-based delivery systems for protein therapeutics and antigens. Adv Drug Deliv Rev Netherlands. 2010;62:59–82.
41. Xiang Y, Liu Y, Mi B, Leng Y. Hydrated polyamide membrane and its interaction with alginate: a molecular dynamics study. Langmuir United States. 2013;29:11600–8.
42. Nafee N, Schneider M, Schaefer UF, Lehr C-M. Relevance of the colloidal stability of chitosan/PLGA nanoparticles on their cytotoxicity profile. Int J Pharm Netherlands. 2009;381:130–9.
43. Rodrigues S, Dionisio M, Lopez CR, Grenha A. Biocompatibility of chitosan carriers with application in drug delivery. J Funct Biomater Switzerland. 2012;3:615–41.
44. Zhao L, Yang G, Shi Y, Su C, Chang J. Co-delivery of Gefitinib and chloroquine by chitosan nanoparticles for overcoming the drug acquired resistance. J Nanobiotechnology England. 2015;13:57.
45. Salatin S, Yari KA. Overviews on the cellular uptake mechanism of polysaccharide colloidal nanoparticles. J Cell Mol Med England. 2017;21:1668–86.
46. Prokop A, Davidson JM. Nanovehicular intracellular delivery systems. J Pharm Sci Elsevier. 2008;97:3518–90.
47. Li Q, Liu C-G, Yu Y. Separation of monodisperse alginate nanoparticles and effect of particle size on transport of vitamin E. Carbohydr Polym England. 2015;124:274–9.